JOC Article
pubs.acs.org/joc

Chemoselective C-4 Aerobic Oxidation of Catechin Derivatives Catalyzed by the *Trametes villosa* Laccase/1-Hydroxybenzotriazole System: Synthetic and Mechanistic Aspects

Roberta Bernini,[†,*] Fernanda Crisante,[†] Patrizia Gentili,[‡,*] Fabio Morana,[‡] Marco Pierini,[§] and Monica Piras[§]

[†]*Dipartimento di Agrobiologia e Agrochimica, Università degli Studi della Tuscia, Via S. Camillo De Lellis, 01100 Viterbo, Italy,* [‡]*Dipartimento di Chimica and IMC-CNR Sezione Meccanismi di Reazione, Università degli Studi La Sapienza, P. le A. Moro 5, I-00185 Roma, Italy, and* [§]*Dipartimento di Chimica e Tecnologia del Farmaco, Università degli Studi La Sapienza, P. le A. Moro 5, I-00185 Roma, Italy*

berninir@unitus.it; patrizia.gentili@uniroma1.it

Received October 6, 2010

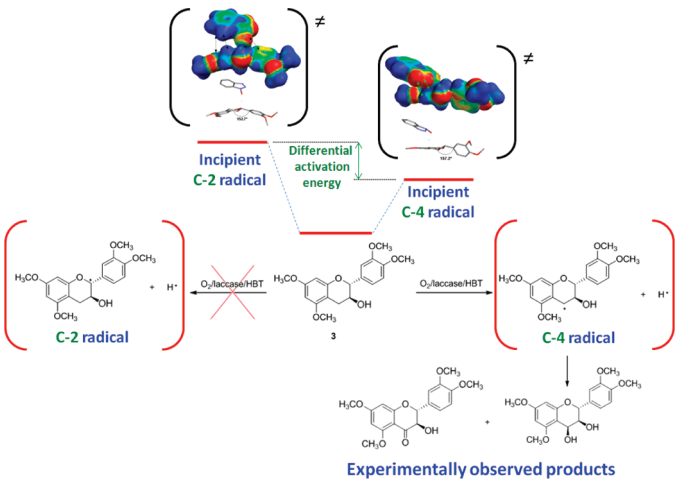

Catechin derivatives were oxidized in air in the presence of the *Trametes villosa* laccase/1-hydroxybenzotriazole (HBT) system in buffered water/1,4-dioxane as reaction medium. The oxidation products, flavan-3,4-diols and the corresponding C-4 ketones, are bioactive compounds and useful intermediates for the hemisynthesis of proanthocyanidins, plant polyphenols which provide beneficial health properties for humans. Determinations of oxidation potentials excluded that catechin derivatives could be directly oxidized by laccase Cu(II), while it resulted in the H-abstraction from benzylic positions being promptly promoted by the enzyme in the presence of the mediator HBT, the parent species producing in situ the reactive intermediate benzotriazole-*N*-oxyl (BTNO) radical. A remarkable and unexpected result for the laccase/HBT oxidative system has been the chemoselective insertion of the oxygen atom into the C-4−H bond of catechin derivatives. Mechanistic aspects of the oxidation reaction have been investigated in detail for the first time in order to corroborate these results. Since the collected experimental findings could not alone provide information useful to clarify the origin of the observed chemoselectivity, these data were expressly supplemented with information derived by suitable molecular modeling investigations. The integrated evaluation of the dissociation energies of the C−H bonds calculated both by semiempirical and DFT methods and the differential activation energies of the process estimated by a molecular modeling approach suggested that the observed selective oxidation at the C-4 carbon has a kinetic origin.

*Authors to whom correspondence should be addressed. Roberta Bernini: phone +39 0761 357452; fax +39 0761 357242 Patrizia Gentili: phone +39 06 49913082; fax +39 490421.

 Published on Web 01/04/2011 DOI: 10.1021/jo101886s

Introduction

Catechins (flavan-3-ols) are phenolic compounds present in a variety of plant foods[1] and beverages, in particular red wine[2] and green tea.[3] Several epidemiological studies have focused on the biological activities, including antioxidant,[4] antibacterial,[5] and anticancer properties,[6] of (+)-catechin **1** and (−)-epicatechin **2** (Figure 1).

These compounds are the building blocks of proanthocyanidins, also known as condensed tannins, flavonoid dimers widely distributed in the plant kingdom.[7] Due to their beneficial health effects,[8] nutritionists and pharmacologists are showing a growing interest in these natural products. Their chemical structure varies depending upon the stereochemistry of the flavan-3-ol starter [2,3-*trans* in (+)-catechin **1** and 2,3-*cis* in (−)-epicatechin **2**] and extension units, the position and stereochemistry of the linkage to the "lower" unit, the degree of polymerization, and the presence or absence of modifications such as esterification of the 3-hydroxyl group. Their biosynthesis is under strict enzymatic control because the different types of dimers are characteristic of specific plant species.[9]

Oxidations of organic compounds are very useful reactions in the fine chemical industry in order to introduce structural chemical modifications into an organic compound and modify its biological and/or pharmacological properties. Stoichiometric toxic oxidants, such as chromium(VI) salts, cerium ammonium nitrate (CAN), thallium(III) nitrate, potassium permanganate ($KMnO_4$), potassium dichromate ($K_2Cr_2O_7$), and sulfuric acid/nitric acid (H_2SO_4/HNO_3), have been widely employed in the past.[10] Recently, according to the green chemistry approach,[11] they have been substituted by ecofriendly reagents, such as oxygen (O_2) and hydrogen peroxide (H_2O_2), activated by an appropriate catalyst (iron and manganese porphyrins, phthalocyanines, iron amide complexes, TAML (Tetra-Amido Macrocyclic Ligand), selenoxides, polyoxometallates, titanium silicalite, tungsten, molybdenum and vanadium complexes, Sn-zeolite beta, and methyltrioxorhenium).[12]

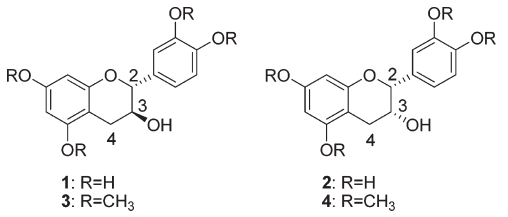

FIGURE 1. Chemical structures of catechin derivatives **1**−**4**.

Some of us have previously reported several oxidative conversions of phenolic compounds into new bioactive compounds by nonenzymatic ecofriendly catalytic oxidations.[13] For example, lactones prepared by oxidative modifications of flavanones exhibited an apoptotic activity on tumoral cell lines;[13a] flavanones obtained from flavones, *p*-benzoquinones from alkylated phenols and catechins were efficient against common strains of saprotrophic soil and seed fungi, pathogenic to humans.[13b−d]

Recently, as an alternative route, we have turned our attention to the oxidations of phenols catalyzed by enzymes. In fact, these compounds are known to be susceptible to enzymatic oxidations giving rise to a variety of dimeric, oligomeric, and polymeric products.[14] Oxidations of phenols by polyphenol oxidase,[15] hydrogen peroxide-dependent peroxidases,[16] and copper oxidases[17] have been described. Polyphenol oxidases, which are involved in the biosynthesis of lignin, tannin, and melanin, catalyze the oxygen-dependent coupling of phenols responsible for browning in fruit juices.[18]

(1) (a) Arts, I. C. W.; Van de Putte, B.; Hollman, P. C. H. *J. Agric. Food Chem.* **2000**, *48*, 1746–1751. (b) Arts, I. C. W.; Al-Awwadi, N.; Bornet, A.; Rouanet, J.-M.; Gasc, F.; Cros, G.; Teissedre, P. L. *Food Res. Int.* **2004**, *37*, 233–245.

(2) (a) Perez-Magarino, S.; Gonzalez-San José, M. L. *J. Agric. Food Chem.* **2004**, *52*, 1181–1189. (b) Xia, E.-Q.; Deng, G.-F.; Guo, Y.-J.; Li, H.-B. *Int. J. Mol. Sci.* **2010**, *11*, 622–646.

(3) (a) Feng, W. Y. *Curr. Drug Metab.* **2006**, *7*, 755–809. (b) Khan, N.; Mukhtar, H. *Life Sci.* **2007**, 519–533. (c) Lambert, J. D.; Sang, S.; Yang, C. S. *Mol. Pharmaceutics* **2007**, *4*, 819–825.

(4) (a) Valcic, S.; Muders, A.; Jacobsen, N. E.; Liebler, D. C.; Timmermann, B. N. *Chem. Res. Toxicol.* **1999**, *12*, 382–386. (b) Bagchi, D.; Bagchi, M.; Bors, W.; Michel, C. *Free Radical Biol. Med.* **1999**, *27*, 1413–1426. (c) Stohs, S. J.; Das, D. K.; Ray, S. D.; Kuszynski, C. A.; Joshi, S. S.; Pruess, H. G. *Toxicology* **2000**, *148*, 187–197. (d) Valcic, S.; Burr, J. A.; Timmermann, B. N.; Liebler, D. C. *Chem. Res. Toxicol.* **2000**, *13*, 801–810. (e) Cren-Olivè, C.; Hapiot, P.; Pinson, J.; Rolando, C. *J. Am. Chem. Soc.* **2002**, *124*, 14027–14038.

(5) Kajiya, K.; Hojo, H.; Suzuki, M.; Nanjo, F.; Kumazawa, S.; Nakayama, T. *J. Agric. Food Chem.* **2004**, *52*, 1514–1519.

(6) Ahmad, N.; Gupta, S.; Mukhtar, H. *Arch. Biochem. Biophys.* **2000**, *376*, 338–346.

(7) (a) Gonzalez-Paramas, A. M.; Esteban-Ruano, S.; Santos-Buelga, C.; De Pascual-Teresa, S.; Rivas-Gonzalo *J. Agric. Food. Chem.* **2004**, *52*, 234–238. (b) Louli, V.; Ragaussis, N.; Magaulas, K. *Bio. Technol.* **2004**, *92*, 201–208.

(8) Xie, D.-Y.; Dixon, R. A. *Phytochemistry* **2005**, *66*, 2127–2144.

(9) (a) Sang, S.; Tian, S. T.; Wang, H.; Stark, R. E.; Rosen, R. T. *Bioorg. Med. Chem.* **2003**, *11*, 3371–3378. (b) Scalbert, A. *Phytochemistry* **1991**, *30*, 3875–3883. (c) Katiyar, S. K.; Mukhtar, H. J. *Cell. Biochem.* **1997**, *27*, 59–67. (d) Dixon, R. A.; De-Yu Xie, D.-Y.; Sharma, S. B. *New Phytol.* **2005**, *165*, 9–28.

(10) Haslam, E. *Phytochemistry* **1977**, *16*, 1625–1640.

(11) Anastas, P.; Eghbali, N. *Chem. Soc. Rev.* **2010**, *39*, 301–312.

(12) (a) Corma, A. In *Fine Chemicals through Heterogeneous Catalysis*; Sheldon, R. A., Van Bekkum, H., Eds.; Wiley-VCH: Weinheim, Germany, 2000; pp 80−91. (b) Jost, C.; Wahl, G.; Kleinhenz, D.; Sundermeyer, J. In *Peroxide Chemistry*; Adam, W., Ed.; Wiley-VCH: Weinheim, Germany, 2000; pp 341−364. (c) Herrmann, W. A. In *Applied Homogeneous Catalysis with Organometallic Compounds*; Cornils, B., Herrmann, W. A., Eds.; Wiley-VCH: Weinheim, Germany, 2002; Vol. 3, pp 1304−1318.

(13) (a) Bernini, R.; Mincione, E.; Cortese, M.; Saladino, R.; Gualandi, G.; Belfiore, M. C. *Tetrahedron Lett.* **2003**, *44*, 4823–4825. (b) Bernini, R.; Mincione, E.; Provenzano, P.; Fabrizi, G. *Tetrahedron Lett.* **2005**, *46*, 2993–2996. (c) Bernini, R.; Mincione, E.; Barontini, M.; Fabrizi, G.; Pasqualetti, M.; Tempesta, S. *Tetrahedron* **2006**, *62*, 7733–7737. (d) Bernini, R.; Mincione, E.; Provenzano, G.; Fabrizi, G.; Tempesta, S.; Pasqualetti, M. *Tetrahedron* **2008**, *64*, 7561–7566.

(14) (a) Cheynier, V.; Osse, C.; Rigaud, J. *J. Food Sci.* **1988**, *53*, 1729–1731. (b) Hirose, Y.; Yamaoka, H.; Nakayama, M. *J. Am. Oil Chem. Soc.* **1991**, *68*, 131–132. (c) Tanaka, T.; Takahashi, M.; Hagino, H.; Nudejima, S.-I.; Usui, H.; Fujii, T.; Taniguchi, M. *Chem. Eng. Sci.* **2009**, *65*, 569–573. (d) Areskogh, D.; Li, J.; Nousiainen, P.; Gellerstedt, G.; Sipilae, J.; Henriksson, G. *Holzforschung* **2010**, *64*, 21–34.

(15) (a) Guyot, S.; Vercauteren, J.; Cheynier, V. *Phytochemistry* **1996**, *42*, 1279–1288. (b) Burton, S. G. *Curr. Org. Chem.* **2003**, *7*, 1317–1331.

(16) (a) Waldemar, A.; Michael, L.; Chantu, R.; Saha, M.; Oliver, W.; Ute, H.; Dietmar, H.; Peter, S. Biotransformations with peroxidases. In *Advances in Biochemical Engineering Biotechnology*; Scheper, T.; Ed.; Springler: New York, 1999; pp 73−108. (b) Adam, W.; Lazarus, M.; Saha-Muller, C. R.; Weichold, O.; Horch, U.; Haring, D.; Schreier, P. Biotransformations with peroxidases. In *Biotrasformations*; Faber, K., Ed.; Springler-Verlag: New York, 2000; pp 73−108. (c) Wilkens, A.; Paulsen, J.; Wray, V.; Winterhalter, P. *J. Agric. Food Chem.* **2010**, *58*, 6754–6761.

(17) (a) Holland, H. L. *Organic Synthesis with oxidative enzymes*; VCH Publishers: New York, 1992; pp 19−24. (b) Queiroz, C.; Mendes Lopes, M. L.; Fialho, E.; Valente-Mesquita, V. L. *Food Rev. Int.* **2008**, *24*, 361–375.

(18) (a) Chenier, V.; Fulcrand, H.; Guyot, S.; Oszmianski, J.; Moutount, M. Reactions of enzymically generated quinones in relation to browing in grape musts and wines. In *Enzymatic browing and its prevention in foods*; Lee, C. Y., Whitaker, J. R., Eds.; ACS Symp. Ser. No. 600; American Chemical Society: Washington, DC, 1995; pp 130−143. (b) Ramirez, E. C.; Whitaker, J. R.; Virador, V. M. Polyphenol oxidase. In *Handbook of Food Enzymology*; Whitaker, J. R., Voragen, A. G. J., Wong, D. W. S., Eds.; Marcel Dekker: New York, 2002, Chapter 39.

SCHEME 1. The Redox Cycle of the Phenolic Oxidase Laccase

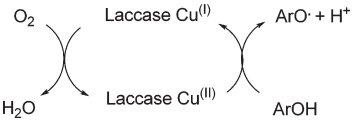

When this biotechnological approach is applied for synthetic purposes, the main practical difficulty is represented by the quantitative isolation of the final products. For example, Shibuya and co-workers described an interesting microbial transformation of (+)-catechin **1** and (−)-epicatechin **2** by an endophytic filamentous fungus *Diaporthe* sp. isolated from the stems of the tea plant *Camellia sinensis*, cultivated in Indonesia. The corresponding biotransformated compounds (flavan-3,4-diols) were obtained at a yield of only 45% and 39%, respectively, together with the recovered catechin (8.5%) and epicatechin (2.4%), indicating a discrete loss of starting materials.[19] Despite the lack of literature data, in order to perform new oxidative modifications of catechin derivatives under mild conditions, on the basis of previous extensive mechanistic studies of some of us,[20] laccase was the enzyme of choice.

Laccase, a class of "blue copper" oxidases excreted by *Basidiomycetes*,[21] contains four copper ions (one T1 copper and a T2/T3 trinuclear copper cluster)[22] and cooperates with other enzymes in the biodelignification process.[23] Four molecules of a reducing substrate are oxidized by this enzyme coupled to the four-electron reduction of oxygen to water.[24] In view of the low redox potential of the T1 Cu(II) site [0.5−0.8 V vs the normal hydrogen electrode (NHE) depending on the fungal source],[25] laccase typically oxidizes phenols (Scheme 1) or phenolic lignin units, due to matching redox features.[26] Electron abstraction and subsequent deprotonation give rise to phenoxyl radicals which undergo oligomerization or cleavage of the aromatic ring upon dioxygen attack.[27]

SCHEME 2. The Radical H-Atom Transfer (HAT) Route of Oxidation of a Benzylic Substrate by the Laccase/HBT System

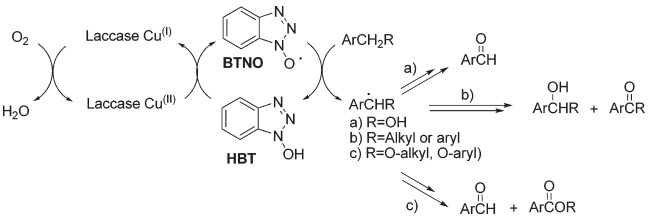

Several examples of polymerization of lignin-related substrates leading to the formation of lignin-analogue polymers are described in the literature.[28] In recent years, the precise control of laccase-catalyzed polymerization of phenolic compounds has garnered attention due to its environmentally benign process for the synthesis of new bioactive polymers, using oxygen or air instead of hydrogen peroxide as oxidizing agent. Examples are poly(catechin) and poly(allylamine)-catechin conjugate exhibiting antioxidant properties.[29]

Substrates having redox potentials above 1.3 V (e.g., benzylic alcohols and ethers)[30] are more resistant to the monoelectronic oxidation and are not oxidized by laccase directly. Indeed, their high redox potential is beyond the electron-abstraction reach of laccase and prevents the occurrence of monoelectronic oxidation. However, in the presence of suitable compounds, namely redox mediators,[31] laccase is able to indirectly oxidize these substrates.[20,32] Among the most common mediators, 1-hydroxybenzotriazole (HBT) is very efficient toward benzylic substrates. Following monoelectronic oxidation by the enzyme, the oxidized mediator [benzotriazole-*N*-oxyl (BTNO) radical] reacts with benzylic alcohol and ether derivatives according to a radical H-abstraction (HAT) route, a mechanism unattainable to laccase. The final products of oxidation depend on the nature of the substrate (Scheme 2).[32]

On the basis of this literature, in this paper we describe our recent results on the oxidative C-4 functionalization of catechin and epicatechin derivatives by using air as oxidant and the *Trametes villosa* laccase/HBT as catalytic system in

(19) (a) Shibuya, H.; Agusta, A.; Ohashi, K.; Maehara, S.; Simanjuntak, P. *Chem. Pharm. Bull.* **2005**, *53*, 866–867. (b) Agusta, A.; Maehara, S.; Ohashi, K.; Simanjuntak, P.; Shibuya, H. *Chem. Pharm. Bull.* **2005**, *53*, 1565–1569.

(20) (a) Baiocco, P.; Barreca, A. M.; Fabbrini, M.; Galli, C.; Gentili, P. *Org. Biomol. Chem.* **2003**, *1*, 191–197. (b) Fabbrini, M.; Galli, C.; Gentili, P. *J. Mol. Catal. B: Enzym.* **2002**, *16*, 231–240.

(21) (a) Messerschmidt, A. *Multi-copper Oxidases*; Word Scientific: Singapore, 1997. (b) Claus, H. *Micron* **2004**, *35*, 93–96. (c) Riva, S. *Trends Biotechnol.* **2006**, 219–226. (d) Witayakran, S.; Ragauskas, A. J. *Adv. Synth. Catal.* **2009**, *351*, 1187–1209. (e) Rodgers, C. J.; Blanford, C. F.; Giddens, S. R.; Skamnioti, P.; Armstrong, F. A.; Gurr, S. J. *Trends Biotechnol.* **2010**, *28*, 63–72.

(22) (a) Solomon, E. I.; Sundaram, U. M.; Machonkin, T. E. *Chem. Rev.* **1996**, *96*, 2563–2605. (b) Solomon, E. I.; Szilagyi, R. K.; DeBeer George, S.; Basumallick, L. *Chem. Rev.* **2004**, *104*, 419–458.

(23) (a) Eriksson, K. E. L. *Biotechnology in the Pulp and Paper Industry. Advances in Biochemical Engineering Biotechnology*; Springer: Berlin, Germany, 1997; Vol. 57, Chapter 2. (b) Reid, I. D.; Paice, M. G. *FEMS Microbiol. Rev.* **1994**, *13*, 369–376. (c) Martinez, A. T.; Speranza, M.; Ruiz-Duenas, F. J.; Ferreira, P.; Camarero, S.; Guillén, F.; Martinez, M. J.; Gutiérrez, A.; del Rio, J. C. *Int. Microbiol.* **2005**, *8*, 195–204.

(24) (a) Yoon, J.; Mirica, L. M.; Stack, T. D. P.; Solomon, E. I. *J. Am. Chem. Soc.* **2005**, *127*, 13680–13693. (b) Quintanar, L.; Yoon, J.; Aznar, C. P.; Palmer, A. E.; Andersson, K. K.; Britt, R. D.; Solomon, E. I. *J. Am. Chem. Soc.* **2005**, *127*, 13832–13845.

(25) (a) Xu, F.; Shin, W.; Brown, S. H.; Wahleithner, J. A.; Sundaram, U. M.; Solomon, E. I. *Biochim. Biophys. Acta* **1996**, *1292*, 303–311. (b) Xu, F.; Palmer, A. E.; Yaver, D. S.; Berka, R. M.; Gambetta, G. A.; Brown, S. H.; Solomon, E. I. *J. Biol. Chem.* **1999**, *274*, 12372–12375. (c) Li, H.; Ewbb, S. P.; Ivanic, J.; Jensen, J. H. *J. Am. Chem. Soc.* **2004**, *126*, 8010–8019.

(26) (a) Astolfi, P.; Brandi, P.; Galli, C.; Gentili, P.; Gerini, M. F.; Greci, L.; Lanzalunga, O. *New J. Chem.* **2005**, *29*, 1308–1317. (b) Gamelas, J. A. F.; Tavares, A. P. M.; Evtuguin, D. V.; Xavier, A. M. B. *J. Mol. Catal. B: Enzym.* **2005**, *33*, 57–64.

(27) (a) Mihailovic, M. L.; Cekovic, Z.; Patai, S. *The Chemistry of the Hydroxyl Group, Part I*; Interscience: New York, 1971; pp 505−592. (b) Ikeda, R.; Sugihara, I.; Uyama, N.; Kobayashi, S. *Macromolecules* **1996**, *29*, 8702–8705. (c) Matsushita, M.; Kamat, K.; Yamaguchi, K.; Mizuno, N. *J. Am. Chem. Soc.* **2005**, *127*, 6632–6640. (d) Schmidt, H. W.; Haemmerli, S. D.; Shoemaker, H. E.; Leisola, M. S. A. *Biochemistry* **1989**, *28*, 1776–1783.

(28) Huttermann, A.; Herche, C.; Haars, A. *Holzforschung* **1980**, *34*, 64–68.

(29) (a) Chung, J. E.; Kurisawa, M.; Tachibana, Y.; Uyama, H.; Kobayashi, S. *Chem. Lett.* **2003**, *32*, 620–621. (b) Kurisawa, M.; Chung, J. C.; Kobayashi, S. *Macromol. Biosci.* **2003**, *3*, 758–764. (c) Osman, A. M.; Wong, K. K. Y.; Fernyhough, A. S.; Rotorua, N. Z. *Enzyme Microb. Technol.* **2007**, *40*, 1272–1279. (d) Itoh, N.; Katsube, Y.; Yamamoto, K.; Nakajima, N.; Yoshida, K. *Tetrahedron* **2007**, *63*, 9488–9492. (e) Ma, H.-L.; Kermasha, S.; Gao, J.-M.; Borges, R. M.; Yu, X.-Z. *J. Mol. Catal. B: Enzym.* **2009**, *57*, 89–95.

(30) Branchi, B.; Galli, C.; Gentili, P. *Org. Biomol. Chem.* **2005**, 2604–2614.

(31) (a) Bourbonnais, R.; Paice, M. G. *FEBS Lett.* **1990**, *267*, 99–102. (b) Call, H. P.; Mücke, I. *J. Biotechnol.* **1997**, *53*, 163–202.

(32) (a) D'Acunzo, F.; Baiocco, P.; Fabbrini, M.; Galli, C.; Gentili, P. *Eur. J. Org. Chem.* **2002**, 4195–4201. (b) D'Acunzo, F.; Baiocco, P.; Galli, C. *New J. Chem.* **2003**, *27*, 329–332. (c) Cantarella, G.; Galli, C.; Gentili, P. *J. Mol. Catal. B: Enzym.* **2003**, *22*, 135–144.

SCHEME 3. Oxidation Reaction of Catechin 5,7,3′,4′-Tetramethyl Ether 3 with O_2/Laccase/HBT

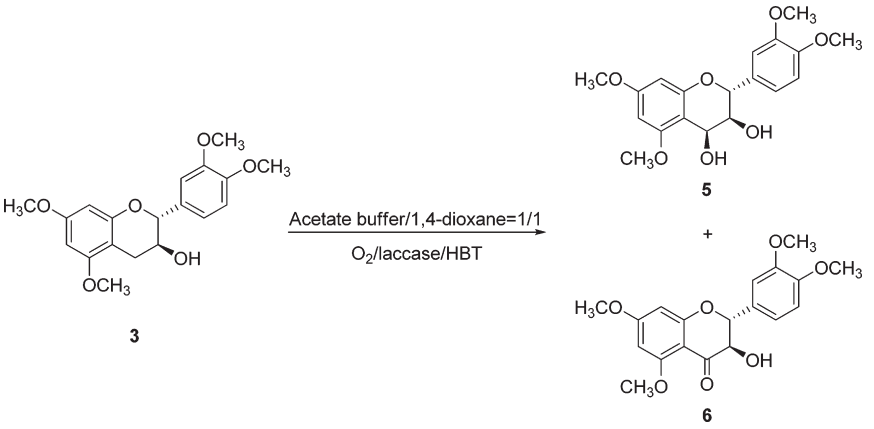

TABLE 1. Experimental Conditions of the Oxidation Reaction Depicted in Schemes 3−5

entry	substrate	substrate (μmol)/HBT (μmol)/laccase (Units)	reaction time (h)	conv (%)[a]	yield (%)[b]
1	**3**	6/0/1	24		
2	**3**	6/0/1	50		
3	**3**	6/0/1	72		
4	**3**	6/2/1	24	50	**5**: 10; **6**: 35
5	**3**	6/2/1	50	75	**5**: 21; **6**: 48
6	**3**	6/2/1	72	77	**5**: 22; **6**: 53
7	**3**	1/1/1	50	75	**5**: 11; **6**: 61
8	**3**	1/1/1	72	76	**5**: 15; **6**: 65
9	**7**	6/2/1	50	78	**8**: 26; **9**: 46
10	**4**	6/2/1	50	80	**10**: 38; **11**: 13

[a]Calculated by HPLC analyses. [b]Yields (±2%) were reckoned vs the molar amount of substrate; the difference to 100% was substrate recovered.

aqueous reaction medium. Experimental and computational data have been integrated in order to explain the observed chemoselectivity of the C-4 oxidation.

Results and Discussion

1. Synthetic Aspects. As previously reported, catechin derivatives polymerize in the presence of laccase.[29] To avoid this reaction, we derivatized the phenolic groups of (+)-catechin **1** and (−)-epicatechin **2** by a methylation reaction obtaining the corresponding 5,7,3′,4′-tetramethyl ethers **3** and **4** in quantitative yield.[13b,33]

As reported in Scheme 2 (path b), previous synthetic and mechanistic investigations showed that the radical oxidation of benzyl ethers[32b] and alkyl arenes[32c] performed by the laccase/HBT system gave rise to the corresponding alcohols and ketones, both deriving from the oxidation at the benzylic position. A carbon radical originating from the cleavage of the benzylic C−H bond of the substrate was the key intermediate in the oxidation process. On the basis of these experimental data, we hypothesized that the laccase/HBT system would accomplish the insertion of an oxygen atom in C-2 and/or C-4 of catechin derivatives (Figure 1).

Generally, oxidation reactions with laccase were performed in buffered water at pH 4.5−5.0. As expected, under these experimental conditions, catechin derivatives **3** and **4** were insoluble. The reaction medium able to both solubilize **3** and **4** and retain the activity of laccase was the mixture sodium acetate buffer/1,4-dioxane (1/1, v/v). As reported in the literature,[34] under these experimental conditions, laccase retained at least 75% of its activity determined in aqueous buffer (5277 Unit/mL). In this mixed solvent, we performed the oxidation reaction of catechin 5,7,3′,4′-tetramethyl ether **3** under different experimental conditions (Scheme 3, Table 1).

In the absence of HBT the oxidation reaction did not proceed and the substrate was quantitatively recovered (Table 1, entries 1−3). On the contrary, in the presence of HBT, we observed the formation of two oxidation products **5** and **6** regardless of reaction conditions, together with unreacted substrate (Table 1, entries 4−8). Satisfactory results in terms of substrate conversion and product yield were obtained by using a ratio of substrate/HBT/laccase = 6/2/1 and performing the oxidation for 50 h (Table 1, entry 5). Prolonging the reaction time until 72 h, no significant differences in terms of conversion and yield were observed (Table 1, entry 6). Changing the ratio of substrate/HBT/laccase (1/1/1) resulted in an increase of the yield of compound **6** and a decrease of the yield of **5** (Table 1, compare entry 5 with entry 7). Furthermore, we did not observe a complete conversion of **5** into **6** after 72 h and the ratio between compounds **5** and **6** was not significantly changed (Table 1, entry 8).

Oxidation products **5** and **6** were isolated after chromatographic purification on silica gel and characterized by spectroscopic analyses. The ^{1}H NMR spectrum of compound **5** suggested that it was a flavan-3,4-diol with 2,3-*trans*-3,4-*cis*

(33) (a) Hori, K.; Satake, T.; Saiki, Y.; Murakami, T.; Chen, C.-M. *Chem. Pharm. Bull.* **1988**, *36*, 4301–4306. (b) Liu, H.; Yamazaki, Y.; Sasaki, T.; Uchida, M.; Tanaka, H.; Oka, S. *Phytochemistry* **1999**, *51*, 297–308.

(34) D'Acunzo, F.; Barreca, A. M.; Galli, C. *J. Mol. Catal. B: Enzym.* **2004**, *31*, 25–30.

SCHEME 4. Oxidation Reaction of 3-*O*-Acetyl-catechin 5,7,3′,4′-Tetramethyl Ether 7 with O_2/Laccase/HBT

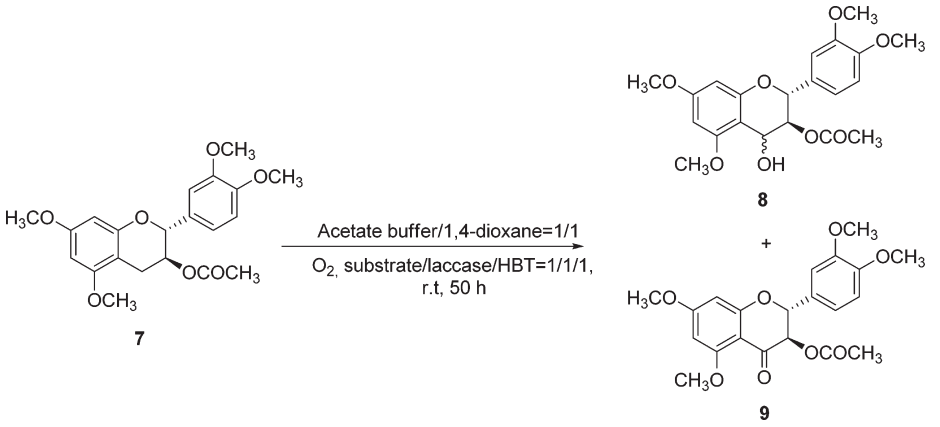

stereochemistry ($J_{2,3}$ = 10.0 Hz and $J_{3,4}$ = 4.2 Hz);[19,35] compound **6** was identified as the corresponding C-4 ketone (taxifolin 5,7,3′,4′-tetramethyl ether).[35] To the best of our knowledge, this is the first study to report the benzylic aerobic oxidation of catechin derivatives catalyzed by the laccase/HBT system. This procedure appears to be a valid alternative to the use of harsh chemical reagents such as 2,3-dichloro-5,6-dicyano-1,4-benzoquinone (DDQ)[36] and lead(IV) acetate.[37] On the basis of the assignments of compounds **5** and **6**, we could conclude that the laccase/HBT system oxidized the C-4 position of (+)-catechin 5,7,3′,4′-tetramethyl ether **3** with a complete chemo- and stereoselectivity. In fact, no C-2 oxidation products were observed; the oxygen was inserted in the *sin* position with respect to the hydroxyl group present in C-3.

With the aim of evaluating a possible role played by the hydroxyl group bonded to C-3 in directing the oxidation reaction at the C-4 position, we performed the oxidation with oxygen/laccase/HBT of 3-*O*-acetyl-catechin 5,7,3′,4′-tetramethyl ether **7** (Scheme 4), previously prepared by acetylation of **3** with acetic anhydride in pyridine.[38]

In the presence of oxygen/laccase/HBT = 6/2/1, after 50 h (Table 1, entry 9), we observed that the insertion of the oxygen atom proceeded exclusively in C-4, giving rise to flavan-4-ol **8** (yield 26%) and ketone **9** (yield 46%).[39] Unfortunately, we could not assign any configuration to the hydroxyl group inserted in C-4 of compound **8**, being the ^{1}H NMR signals of protons in C-3 and C-4 are not resolved.

Finally, we performed the oxidation of epicatechin 5,7,3′,4′-tetramethyl ether **4** in the same experimental conditions (Scheme 5).

In this case, the crude reaction was more complex and the chromatographic purification proved to be more difficult probably due to the instability of some of the oxidation

SCHEME 5. Oxidation Reaction of Epicatechin 5,7,3′,4′-Tetramethyl Ether 4 with O_2/Laccase/HBT

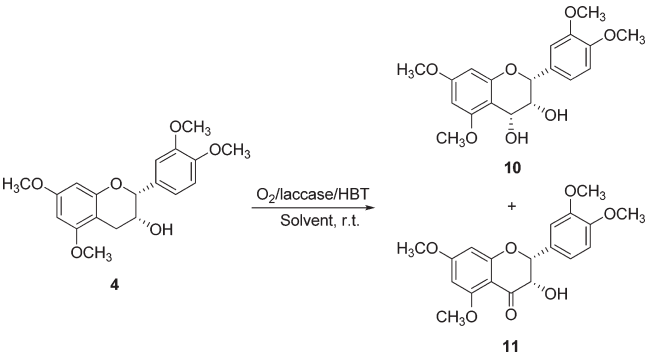

products. Then, under these conditions, we were able to isolate only compounds **10** and **11** (Table 1, entry 10). On the basis of the ^{1}H NMR spectrum, compound **10** was assigned as the 2,3-*cis*-3,4-*cis*-flavan-3,4-diol ($J_{2,3}$ = 1.2 Hz and $J_{3,4}$ = 3.0 Hz);[19,35] compound **11** was the corresponding C-4 ketone (epitaxifolin 5,7,3′,4′-tetramethyl ether).[19,35]

We could not conclude that in this case the oxidation reaction proceeded exclusively at the C-4 position, but without any doubt we could affirm that the oxidation proceeded *preferentially* at this position as the oxidation products accounted for 64% of the total converted substrate.

Flavan-3,4-diols **5**, **8**, and **10** and the corresponding C-4 ketones **6**, **9**, and **11** are useful phenolic compounds. In fact, they are the building blocks in the hemisynthesis of proanthocyanidins.[40] Furthermore, C-4 ketones **6**, **9**, and **11** are structurally related to taxifolin and epitaxifolin, flavonoids exhibiting many beneficial health activities (antioxidant, antiviral, antitumoral, anti-inflammatory)[41,42]

(35) (a) Baig, M. I.; Clark-Lewis, J. W.; Jemison, R. W.; Thompson, M. *J. Chem. Commun.* **1969**, 820–821. (b) Baig, M. I.; Clark-Lewis, J. W.; Thompson, M. *Aust. J. Chem.* **1969**, *22*, 2645–2650. (c) Takahashi, H.; Li, S.; Harigaya, Y.; Onda, M. *J. Nat. Prod.* **1988**, *51*, 730–735.

(36) Steenkamp, J. A.; Ferreira, D.; Roux, D. G. *Tetrahedron Lett.* **1985**, *26*, 3045–3048.

(37) (a) Bokadia, M. M.; Brown, B. R.; Cummings, W. *J. Chem. Soc.* **1960**, 3308–3313. (b) Betts, M. J.; Brown, B. R.; Shaw, M. R. *J. Chem. Soc.* **1969**, 1178–1184. (c) Kawamoto, H.; Nakatsubo, F.; Murakami, K. *Mokuzia Gakkaishi* **1991**, *37*, 741–747.

(38) van Rensburg, H.; van Heerden, P. S.; Ferreira, D. *J. Chem. Soc., Perkin Trans. 1* **1997**, 3415–3421.

(39) Clark-Lewis, J. W.; Thompson, M. *Aust. J. Chem.* **1968**, *21*, 3015–3022.

(40) (a) Delcour, J. A. *J. Chem. Soc., Perkin Trans. I* **1983**, 1711–1717. (b) Balas, L.; Vercauteren, J. *Magn. Reson. Chem.* **1994**, *32*, 386–393. (c) Salas, E.; Atanasova, V.; Poncet-Legarn, C.; Meudee, E.; Mazauric, J. P.; Cheynier, V. *Anal. Chim. Acta* **2004**, *513*, 325–332. (d) Trouillas, P.; Fagnere, C.; Lazzaroni, R.; Calliste, C.; Marfak, A.; Duroux, J.-L. *Food Chem.* **2004**, *88*, 571–582.

(41) Willfor, S. M.; Ahoutupa, M. O.; Hemming, J. E.; Reunanen, M. H. T.; Eklund, P. C.; Sjoholm, R. E.; Eckerman, C. S. E.; Pohjamo, S.; Holmbom, B. R. *J. Agric. Food Chem.* **2003**, *51*, 7600–7606.

(42) (a) Wen, X.; Walle, T. *Drug Metab. Dispos.* **2006**, *34*, 1786-1792; (b) Tsuji, P. A.; Walle, T. *Carcinogenesis* **2006**, *27*, 1579–1585. (c) Walle, T. *Semin. Cancer Biol.* **2007**, *17*, 354–362. (d) Walle, T.; Ta, N.; Kawamori, T.; Wen, X.; Tsuji, P. A.; Walle., U. K. *Biochem. Pharmacol.* **2007**, *73*, 1288–1296.

TABLE 2. Oxidation Potential and Dissociation Energies of C-2−H and C-4−H Bonds of Catechin Derivatives 3, 4, and 7

		BDE_{C-H} (kJ mol^{-1})						
substrate	E^p (V, vs NHE)[a]	AM1[b]	error	B3LYP/6-31G*//AM1)[b]	error	B3LYP/6-311+G**//AM1[b]	error	tabulated data[c]
$\mathbf{3}_{C-2}$	6.9	296.6				377.4		
$\mathbf{3}_{C-4}$		306.7				378.2		
$\mathbf{4}_{C-2}$	6.9	290.4		366.1		367.4		
$\mathbf{4}_{C-4}$		306.7		377.0		376.6		
$\mathbf{7}_{C-2}$	7.2	298.6				386.6		
$\mathbf{7}_{C-4}$		301.4				381.2		
12		296.2	62.8	361.5	−2.5	358.6	0.4	359.0
13		318.8	54.0	393.3	−20.5	387.4	−14.6	372.8
14		301.2	57.8	360.7	−1.7	355.6	3.3	359.0
15		318.0	60.7	392.5	−13.8	387.0	−8.4	378.6
$\mathbf{16}_{C-H1}$		297.5	61.5	368.6	−9.6	367.8	−8.8	359.0
$\mathbf{16}_{C-H2}$		301.7	71.1	383.2	−10.5	379.5	−6.7	372.8
17		301.7				359.8		
18		315.5				387.9		
av error on the calcd BDE_{C-H} data (kJ mol^{-1})			61.3		9.8		7.0	

[a][Substrate]: 2 mM, at 500 mV/s in CH_3CN containing Bu_4NF (0.1 M). [b]From the following equation: $BDE_{C-H} = \Delta H°_f(R) + \Delta H°_f(H) - \Delta H°_f(R-H)$. [c]See ref 43 and 44.

and used in various applications such as cosmetics and supplements.

2. Mechanistic Aspects. a. Oxidation Potential and Bond Dissociation Energies (BDE). As previously reported, catechin derivatives **3**, **4**, and **7** were not oxidized by laccase alone and they were recovered quantitatively even after 50 h of reaction. Determination of the oxidation potential by cyclic voltammetry in acetonitrile containing tetrabutylammonium fluoride as supporting electrolyte indicated that these substrates were irreversibly oxidized at a potential above 1.6 V (Table 2), confirming that they are resistant to monoelectronic oxidation and cannot be oxidized by laccase Cu(II) directly.

When HBT was present as mediator, substrates were oxidized exclusively (or *preferentially*) at the C-4 position (Schemes 3−5). As described in the Introduction, the key step in the oxidation of a substrate by the laccase/HBT system is the abstraction of a hydrogen atom from the benzylic position (Scheme 2). Redox features of the substrate have no major impact upon this radical HAT route, where only the enthalpic balance between the breaking and forming of bonds is relevant.[26a] In the specific case of aminoxyl radical BTNO, the energy of the NO−H bond formed by H-abstraction (356 kJ/mol)[26a] is similar to that of the benzylic C−H bond in several substrates.[45] Moreover, according to this mechanism, the weaker the C−H bond the faster the HAT route, either with BTNO or other radical species. We corroborated this by correlating the energies of activation of the BTNO-induced HAT route with a homologous series of benzylic substrates (alkyl arenes and benzyl alcohols) vs the corresponding BDE_{C-H} data according to the Evans−Polanyi equation ($E_a = \alpha BDE_{C-H} + \text{constant}$).[41] Unfortunately, thermochemical data are not always available in order to attempt a similar correlation and the ensuing rationalization of the reactivity trend. Moreover, Griller et al.[46] demonstrated that hyperconjugation from the lone-pair of a heteroatom weakens an adjacent C−H bond and stabilizes an intervening C-radical generated by H-abstraction. The contribution arising from this effect on the energy destabilization of an adjacent C−H bond is greater than the more colinear C−H bond and the lone-pair are,[47] and this interaction accounts for 29−38 kJ/mol weakening of the C−H bond.

In the present work, in contrast, results reported in Schemes 3−5 clearly indicated that BTNO preferred to abstract a hydrogen atom from the benzylic C-4 position of catechin derivatives **3**, **4**, and **7** rather than from the benzylic C-2 position, taking advantage of the presence of the adjacent oxygen atom. As the thermochemical BDE_{C-H} data for the benzylic positions of catechins **3**, **4**, and **7** were not reported in the literature, we calculated the dissociation energies for both the C-2−H and C-4−H bonds of substrates in order to investigate this chemoselective behavior, as illustrated in Scheme 6.

The BDE_{C-H} values for the H-abstraction from the C-2 or C-4 position of each substrate were estimated by modeling the geometries corresponding to their ground and radical states using the semiempirical method AM1 and afterward evaluating the respective thermochemical stabilities by single point energy calculations performed using the B3LYP DFT method at two different levels of accuracy [the basis sets 6-31G(*) and 6-311+G(**)]. All the obtained results are summarized in Table 2, together with other BDE_{C-H} values calculated for the relevant structures **12**−**18** of Scheme 7 used as models suitable for validation of the approach.

For compounds **12** to **16**, the assessed BDE_{C-H} values have been compared with the thermochemical data reported in the literature,[41,42] while the computed BDE_{C-H} values for compounds **17** and **18** have been used for a qualitative comparison based on their respective tendency to undergo oxidation by the laccase/HBT system.[34]

As can be seen from Table 2, the agreement between the calculated and experimental BDE_{C-H} values clearly increased by passing from the semiempirical to the DFT energetic evaluation, already achieving a good assessment

(43) *Handbook of Chemistry and Physics*, 74 ed.; CRC Press: Cleveland, OH, 1993−1994.
(44) Yu-Ran, L. *Handbook of Bond Dissociation Energies in Organic Compounds*; CRC Press: Cleveland, OH, 2003.
(45) Brandi, P.; Galli, C.; Gentili, P. *J. Org. Chem.* **2005**, *70*, 9521–9528.
(46) Griller, D.; Howard, J. A.; Mariott, P. R.; Scaiano, J. C. *J. Am. Chem. Soc.* **1981**, *103*, 619–623.
(47) Malatesta, V.; Ingold, K. U. *J. Am. Chem. Soc.* **1981**, *103*, 609–614.

employing the less extended basis set 6-31G(*). For the three considered methods AM1, B3LYP/6-31G*//AM1, and B3LYP/6-311+G**//AM1 the averaged absolute errors from the tabulated data (i.e., $|BDE_{C-H}^{exp} - BDE_{C-H}^{calc}|$) were 61.3, 9.8, and 7.0 kJ/mol, respectively. In addition and as expected, when the comparison was performed between the BDE_{C-H} data involving the rupture of different C−H bonds inside the same molecule, the absolute errors arising from the used method tended to cancel one another out. This is in fact evident in the case of compound **16**; the relative difference between the BDE_{C-H} values related to the rupture of bonds C−H_1 and C−H_2 (Scheme 7) inside the same structure differed from the tabulated data by 9.6, 0.8, and 2.1 kJ/mol by passing from the least to the most precise calculation method, respectively. According to these calculation findings, compounds **12**, **14**, $\mathbf{16}_{C-H1}$, and **17**, which are simple models for the generation of a radical at the benzyl position having an adjacent oxygen atom (i.e., carbon C-2) in catechin derivatives, showed lower BDE_{C-H} values than compounds **13**, **15**, $\mathbf{16}_{C-H2}$, and **18**, which are models for the H-abstraction from the C-4 position in the same catechin derivatives (Table 2). In agreement with these results, the values of BDE_{C-H} reported in Table 2 for catechin tetramethyl ethers **3** and **4** indicated an advantage for the H-abstraction from carbon C-2, although for compound **3** this preference was limited (−0.8 kJ/mol by the most accurate method). However, for 3-*O*-acetyl-catechin 5,7,3′,4′-tetramethyl ether **7** the higher level of calculus assessed an inverted order of stability (5.4 kJ/mol in favor of the C-4−H rupture) that could not justify the observed chemoselectivity in quantitative terms. As a further check, we also evaluated the possible effect that the solvent could exercise on the estimation of BDE_{C-H}. For this purpose, using catechin 5,7,3′,4′-tetramethyl ether **3**, we performed a structural optimization of the radicals at carbons C-2 and C-4 by the BLYP/DZP (medium core) method. The solvation energy in 1,4-dioxane (a medium quite similar to the mixture used as solvent for the reaction of Scheme 3) was taken into account by the COSMO procedure, as implemented in the ADF computer program package. The result indicated that the solvent could affect the BDE_{C-H} assessment to a moderate extent ($E\mathbf{3}_{C-2} - E\mathbf{3}_{C-4} = -8.8$ kJ/mol in 1,4-dioxane compared with −11.3 kJ/mol in vacuo).

SCHEME 6. Calculation of C-2−H and C-4−H BDEs for Catechin Derivatives 3, 4, and 7

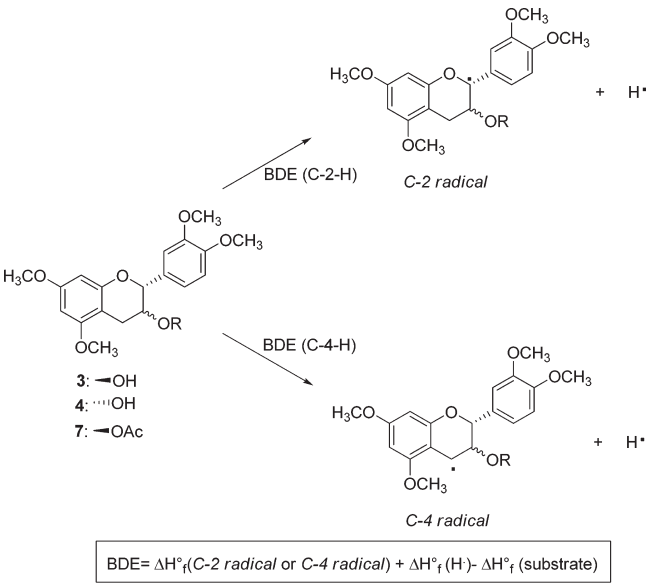

SCHEME 7. Compounds Used As Models of the H-Abstraction from Benzylic Carbons of Catechin Derivatives[a]

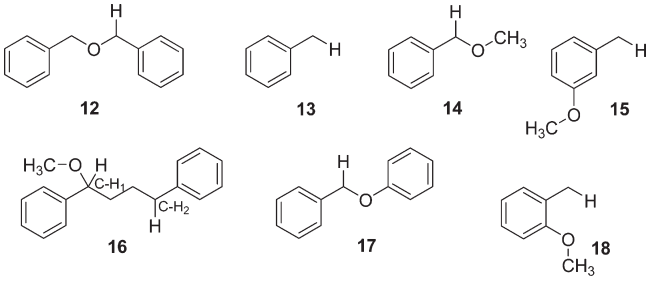

[a]Hydrogen atoms involved in generation of the considered radicals are explicitly depicted.

On the basis of these BDEs and according to the oxidation mechanism by the laccase/HBT system, in all cases the BTNO radical *should* remove a hydrogen atom from *both* C-2 and C-4 carbon atoms, in contrast to the *preferential* exclusive H-abstraction from the C-4−H position as indicated by the experimental distribution of products (Table 1).

b. H-Abstraction Reactivity. To advance our understanding of the reactivity of aminoxyl radical BTNO in the H-abstraction from catechin derivatives **3**, **4**, and **7**, we measured the second-order rate constant k_H of the process (Scheme 8).

The kinetic system has previously been described.[45] Addition of a stoichiometric amount of the monoelectronic oxidant CAN [$(NH_4)_2Ce(NO_3)_6$; $E^\circ = 1.3$ V vs NHE][48] to HBT ($E^\circ = 1.08$ V vs NHE) in acetonitrile solution at 25 °C, both compounds at 0.5 mM initial concentration, gave rise to a broad absorption band in the $\lambda = 350-600$ nm range

SCHEME 8. Kinetic Study of the H-Atom Abstraction from the C−H Bond of Catechin Derivatives 3, 4, and 7

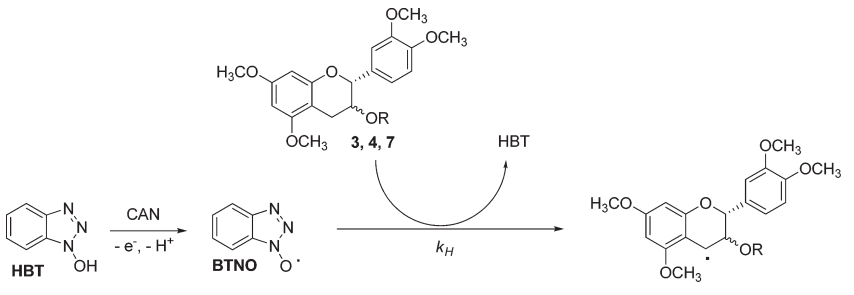

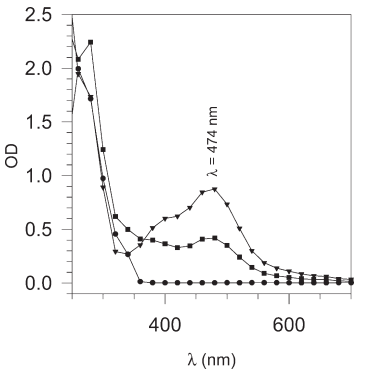

FIGURE 2. UV−vis spectrum of a 0.5 mM solution of HBT in acetonitrile: before the addition of CAN (●); 15 ms after the addition of CAN (0.5 mM) (▲); 110 s after the addition (■).

(Figure 2)[49] having λ_{max} at 474 nm and $\varepsilon = 1840\ M^{-1}\ cm^{-1}$. The band pertained to the formation of the BTNO species; electron transfer from HBT to CAN was in fact exoergonic and occurred quantitatively (Scheme 8). The spectrum of BTNO was not stable but decayed according to an almost first-order exponential curve ($k_{decay} = 5.1 \times 10^{-3}\ s^{-1}$ in MeCN at 25 °C), with a half-life of approximately 140 s at 0.5 mM.[49]

The spontaneous decay of BTNO was greatly accelerated in the presence of purposely added H-donor substrates. By following the progress of the reaction at $\lambda = 474$ nm through stopped-flow spectrophotometry or conventional spectrophotometry, the reactivity of BTNO in the H-abstraction from the C-4−H position of catechin derivatives was investigated for catechin derivatives **3**, **4**, and **7** and for the two model compounds **17** and **18**. For kinetic purposes, the solution of the C−H-bearing substrate was employed at initial concentrations higher than the concentration of BTNO, in order to fulfill the pseudo-first-order kinetic conditions, and the reduction in absorbance at $\lambda = 474$ nm was followed. The pseudo-first-order rate constants k', determined at 25 °C at four to five initial concentrations of substrate from at least duplicated experiments, were converted into second-order H-abstraction rate constants (k_H) by determining the slope of the k' vs $[substrate]_o$ plot, as shown in Figure 3 for catechin 5,7,3′,4′-tetramethyl ether **3**.

The k' constants were faster than the spontaneous decay of BTNO in all cases investigated (as can be seen from the linearity of the plot and the minor y-intercept in Figure 3) and exhibited first-order dependence on the excess substrate concentration. The second-order rate constants (k_H) are given in Table 3 for all the substrates.

The results obtained for benzyl phenyl ether **17** (k_H/number of equivalent H atoms = 0.24 $M^{-1}\ s^{-1}$) and 2-methyl anisole **18** (k_H/number of equivalent H atoms = 0.027 $M^{-1}\ s^{-1}$) were in accordance with the calculated BDEs (359.8 and 387.9 kJ/mol, respectively). Therefore, the substrate with a lower bonding dissociation energy was more prone to hydrogen atom abstraction. In other words, the presence of an oxygen atom weakened the adjacent C−H bond by hyperconjugation between its lone-pair and the

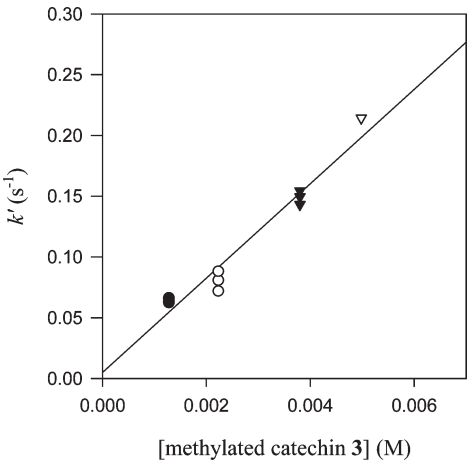

FIGURE 3. Determination of the second-order rate constant k_H for the reaction of BTNO with catechin 5,7,3′,4-tetramethyl ether **3** in acetonitrile at 25 °C from the plot of the pseudo-first-order rate constant k' at various initial concentrations of the substrate.

TABLE 3. Rate Constants k_H Obtained Spectrophotometrically at 25 °C in CH_3CN from Reaction of BTNO with Catechin Derivatives 3, 4, and 7 and Model Compounds 17 and 18[a]

entry	substrate	k_H ($M^{-1}\ s^{-1}$)
1	**3**	38 ± 1
2	**4**	46 ± 1
3	**7**	29 ± 1
4	**17** (2)[b]	0.49 ± 0.04
5	**18** (3)[b]	0.082 ± 0.004

[a]Initial condition: [BTNO] = 0.5 mM, [substrate] = 5−40 mM; determination in triplicate. [b]Number of equivalent H atoms.

incipient C-radical generated by H-abstraction. In contrast, catechin derivatives **3**, **4**, and **7** showed a similar k_H according to an equivalent selectivity for the H-abstraction by BTNO (i.e., the preferential oxidation observed at the C-4−H position in all these substrates). However, none of such results provided in itself direct information useful to clarify the origin of the observed chemoselectivity, so that additional information appeared necessary to shed light on the origin of the unexpected selectivity. As stressed below, they were achieved by resorting to suitable molecular modeling investigations.

c. Rationalization of the Chemoselective Oxidation at the Benzylic Carbon C-4. On the basis of the calculation findings reported in Table 2, the chemoselective rupture of the C−H bond promoted by BTNO at the benzylic carbon C-4 of catechin derivatives **3**, **4**, and **7** could not be interpreted as an event driven by thermodynamic factors. Therefore, with the aim of gaining some more direct indications about the true origin of the observed chemoselectivity, we performed a relevant study of molecular modeling on the oxidation reaction of catechin derivatives **3** and **7**. Our analysis was based on the estimation of the relative energetic barriers with which such substrates achieve the transition states (TS) leading to the respective C-2 and C-4 radicals. With the dual intent of attaining a global picture of the potential energy surface governing the interactions between BTNO and the selected catechin substrates and limiting as much as possible the extent of arbitrariness in the generation of the TS structures leading to catechin radicals at carbons C-2 or C-4,

(48) Prabhakar Rao, G.; Vasudeva Murthy, A. R. *J. Phys. Chem.* **1964**, *68*, 1573–1576.
(49) Galli, C.; Gentili, P.; Lanzalunga, O.; Lucarini, M.; Pedulli, G. F. *Chem. Commun.* **2004**, 2356–2357.

we performed relatively in-depth automatic multiconformational molecular docking simulations between the species constituting the couples **3**, BTNO and **7**, BTNO. According to a well-consolidated procedure,[50] in the first step the more representative geometries of compounds **3** and **7**, obtained by suitable modifications of the six-term cycle containing carbons C-2 and C-4 and optimized through the semiempirical method AM1 (three conformers for **3** and one conformer for **7**, in a window of 15 kJ/mol by the respective global minimum, see Figure 4), were docked as rigid bodies against the single structure of BTNO, exploring the whole potential energy surface of interaction without any aprioristic restriction.

Afterward, the energetically more stable adducts generated by the quoted step were further optimized at the AM1 semiempirical level, leaving their geometries free to change in order to maximize the supramolecular interactions (i.e., allowing the establishment of molecular-induced fits according to a "quasi-flexible" docking procedure). Among the members of the ensembles represented by the final totally relaxed two-body adducts, we selected those endowed with geometries suitable to represent reasonable starting points for the omolitic C−H breaking promoted by BTNO at both the C-2 and C-4 benzylic positions. From these structures, by means of minimal translation and/or rotation movements performed by hand, we modeled the new geometries representing approximate TS for the hydrogen transferring from catechin 5,7,3′,4′-tetramethyl ether **3** or 3-*O*-acetyl-catechin 5,7,3′,4′-tetramethyl ether **7** to radical BTNO, which, in turn, were submitted to optimization. Due to the relatively large number of atoms and different adducts involved with the studied supramolecular systems and according to the recognized ability of semiempirical methods to model TS geometries of acceptable quality,[51] the quoted optimizations were performed using the semiempirical Hamiltonian AM1, while the subsequent evaluation of energy differences between them was performed by carrying out single point energy calculations at the high DFT level B3LYP/6-311+G(**), the same method that proved to be completely reliable in the assessments reported in Table 2. All the obtained results are summarized in Table 4.

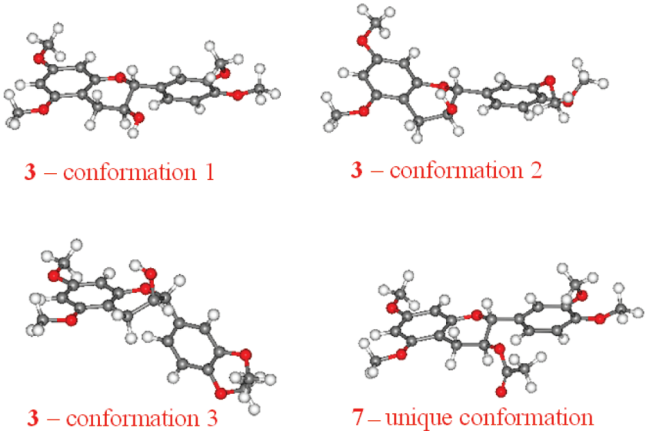

FIGURE 4. Optimized conformers of catechin derivatives **3** and **7**.

c.1. Analysis of the Chemoselective H-Abstraction from the Benzylic Positions of Catechin 5,7,3′,4′-Tetramethyl Ether 3. From the multiconformational "quasi-flexible" docking procedure performed between compound **3** and BTNO, after selection driven by both geometric and energetic criteria,[51] 103 different adducts were obtained inside an energetic window of 13 kJ/mol with respect to the global minimum. From such an ensemble, we identified two clusters of geometries responding to the requisite to be reasonable starting states (or very close to them) for the hydrogen abstraction promoted by the radical BTNO. Their two most stable members, hereafter named $\mathbf{3}_{(C\text{-}2/C\text{-}4)}$-BTNO and $\mathbf{3}_{(C\text{-}2)}$-BTNO, are depicted in Figure 5.

A suitable geometry manipulation followed by semiempirical optimizations of these structures (a detailed description step by step of the adopted procedure is given in Supporting Information) led to three reliable TS (the geometries TS_$\mathbf{3}_{(C\text{-}2)}$-BTNO, TS_$\mathbf{3}_{(C\text{-}4)}$-BTNO_1, and TS_$\mathbf{3}_{(C\text{-}4)}$-BTNO_2 of Figure 5) confirmed by the presence among the evaluated vibrational modes of only one imaginary frequency, corresponding to the migration of the hydrogen from the benzylic carbon C-2 or C-4 of **3** to BTNO. The subsequent estimation of the relative different stability of such TS, performed at the DFT level B3LYP/6-311+G(**), afforded an energetic gap ($\Delta\Delta E^{\#}$) of 15.5 kJ/mol in favor of the H-abstraction from C-4 (difference of energy between TS_$\mathbf{3}_{(C\text{-}2)}$-BTNO and TS_$\mathbf{3}_{(C\text{-}4)}$-BTNO_2). In contrast to the conclusions inferred by reviewing the thermodynamic data reported in Table 2 and relative to the differential stability of the radicals $\mathbf{R3}_{(C\text{-}2)}$ and $\mathbf{R3}_{(C\text{-}4)}$, this result completely agreed with the hypothesis that the observed chemoselective oxidation of **3** is driven by kinetic factors.

TABLE 4. Calculated Energies of Two-Body Adducts between Catechin Derivatives 3, 7, and BTNO and Their Relevant Transition States

	AM1		B3LYP/6-31G*//AM1		B3LYP/6-311+G**//AM1	
substrate	energy (kJ mol^{-1})	$\Delta\Delta E^{\#}$ (kJ mol^{-1})[a]	energy (au)	$\Delta\Delta E^{\#}$ (kJ mol^{-1})[a]	energy (au)	$\Delta\Delta E^{\#}$ (kJ mol^{-1})[a]
$\mathbf{3}_{(C\text{-}2/C\text{-}4)}$-BTNO	−254.0					
$\mathbf{3}_{(C\text{-}2)}$-BTNO	−242.2					
TS_$\mathbf{3}_{(C\text{-}2)}$-BTNO	−121.0	0.8	−1658.89726	11.3 (−5.9)[b]	−1659.35207	15.5
TS_$\mathbf{3}_{(C\text{-}4)}$-BTNO_1	−122.0		−1658.90155		−1659.35791	
TS_$\mathbf{3}_{(C\text{-}4)}$-BTNO_2	−120.1		−1658.89547		−1659.35602	
$\mathbf{7}_{(C\text{-}4cis)}$-BTNO	−403.3					
$\mathbf{7}_{(C\text{-}4trans)}$-BTNO	−401.2					
$\mathbf{7}_{(C\text{-}2)}$-BTNO	−400.8					
TS_$\mathbf{7}_{(C\text{-}2)}$-BTNO	−260.2	3.3	−1811.55257	37.2 (15.9)[b]	−1812.04430	39.3
TS_$\mathbf{7}_{(C\text{-}4cis)}$-BTNO_1	−263.6		−1811.56676		−1812.05920	
TS_$\mathbf{7}_{(C\text{-}4cis)}$-BTNO_2	−261.9		−1811.56496		−1812.05123	
TS_$\mathbf{7}_{(C\text{-}4trans)}$-BTNO	−257.7		−1811.55800		−1812.05124	

[a] $\Delta\Delta E^{\#}$ = (C-2−H − C-4−H) energy differences. [b] Energetic differences between the structures deprived of the BTNO component.

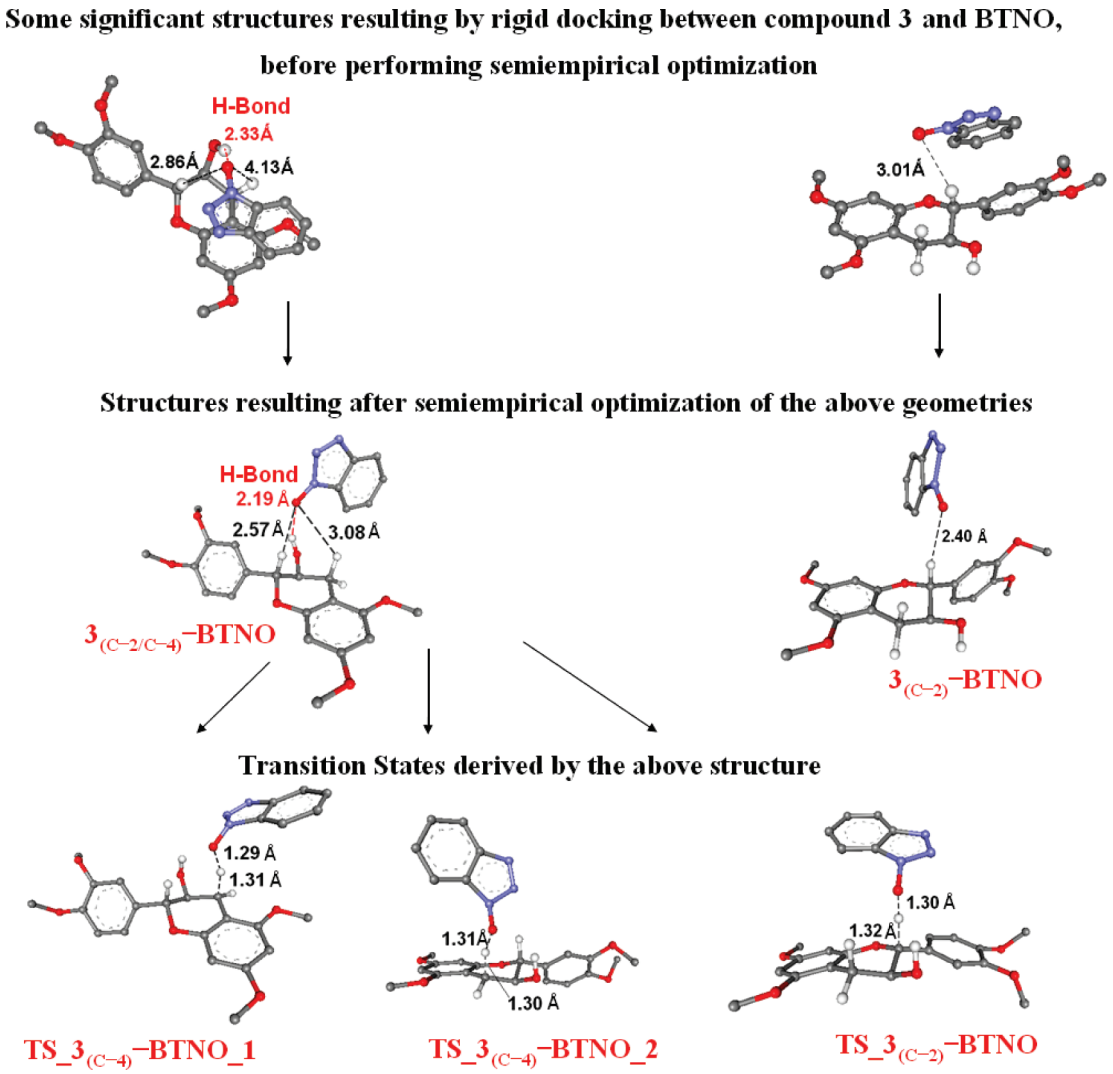

FIGURE 5. Geometries of adducts between catechin 5,7,3′,4′-tetramethyl ether **3** and BTNO, obtained by docking simulation, and related transition states for the hydrogen transfer from compound **3** to BTNO. For the sake of clarity the only hydrogen atoms shown in the picture are those bonded to carbons C-2 and C-4 and to the oxygen belonging to the hydroxyl group.

c.2. Analysis of the H-Abstraction from the C-2 and C-4 Benzylic Positions of 3-*O*-Acetyl-5,7,3′,4′-catechin Tetramethyl Ether 7. By utilizing the same computational approach described for the case of compound **3**, we extended the analysis of the oxidation promoted by BTNO to 3-*O*-acetyl-5,7,3′,4′-catechin tetramethyl ether **7**. The multiconformational docking procedure afforded 40 adducts within an energetic window of 13 kJ/mol involving the species **7** and BTNO. In turn, from this ensemble it was possible to identify three clusters of adducts endowed with geometries reasonably consistent with hypothetical starting states for the hydrogen abstraction triggered by the radical BTNO. The two most stable of them had the BTNO close to the hydrogen atoms bonded at carbon C-4 (the $\mathbf{7}_{(C\text{-}4cis)}$-BTNO and $\mathbf{7}_{(C\text{-}4trans)}$-BTNO geometries reported in Figure 6), whereas, in the most stable structure of the third cluster, BTNO had its oxygen near the hydrogen bonded at carbon C-2 (the $\mathbf{7}_{(C\text{-}2)}$-BTNO adduct). More specifically, in $\mathbf{7}_{(C\text{-}4cis)}$-BTNO the C-4-H hydrogen susceptible to abstraction by BTNO was *cis* to the hydrogen on C-2, whereas in $\mathbf{7}_{(C\text{-}4trans)}$-BTNO the migrant hydrogen was *trans*.

As already described about the adducts formed between catechin **3** and BTNO, also in the present case a suitable structural manipulation of the complexes found by docking analysis (details concerning the steps of the procedure are available in Supporting Information), followed by semiempirical optimization afforded the related transition states TS_$\mathbf{7}_{(C\text{-}2)}$-BTNO, TS_$\mathbf{7}_{(C\text{-}4cis)}$-BTNO, and TS_$\mathbf{7}_{(C\text{-}4trans)}$-BTNO (the TS nature of such structures was validated by analysis of the relevant vibrational modes).

(50) (a) Alcaro, S.; Gasparrini, F.; Incani, O.; Mecucci, S.; Misiti, D.; Pierini, M.; Villani, C. *J. Comput. Chem.* **2000**, *21*, 515–530. (b) Alcaro, S.; Gasparrini, F.; Incani, O.; Caglioti, L.; Pierini, M.; Villani, C. *J. Comput. Chem.* **2007**, *28*, 1119–1128. (c) Filippi, A.; Gasparrini, F.; Pierini, M.; Speranza, M.; Villani, C. *J. Am. Chem. Soc.* **2005**, *127*, 11912–11913. (d) Gasparrini, F.; Pierini, M.; Villani, C.; Filippi, A.; Speranza, M. *J. Am. Chem. Soc.* **2008**, *130*, 522–534. (e) Siani, G.; Angelini, G.; De Maria, P.; Fontana, A.; Pierini, M. *Org. Biomol. Chem.* **2008**, *6*, 4236–4241. (f) Fraschetti, C.; Pierini, M.; Villani, C.; Gasparrini, F.; Levi Mortera, S.; Speranza, M. *Chem. Commun.* **2009**, 5430–5432.

(51) (a) Hehre, W. J. *Practical Strategies for Electronic Structure Calculations*; Wavefunction, Inc.: Irvine, CA, 1995. (b) Hehre, W. J.; Shusterman, A. J.; Huang, W. W. *A Laboratory Book of Computational Organic Chemistry*;, Wavefunction, Inc.: Irvine, CA, 1996.

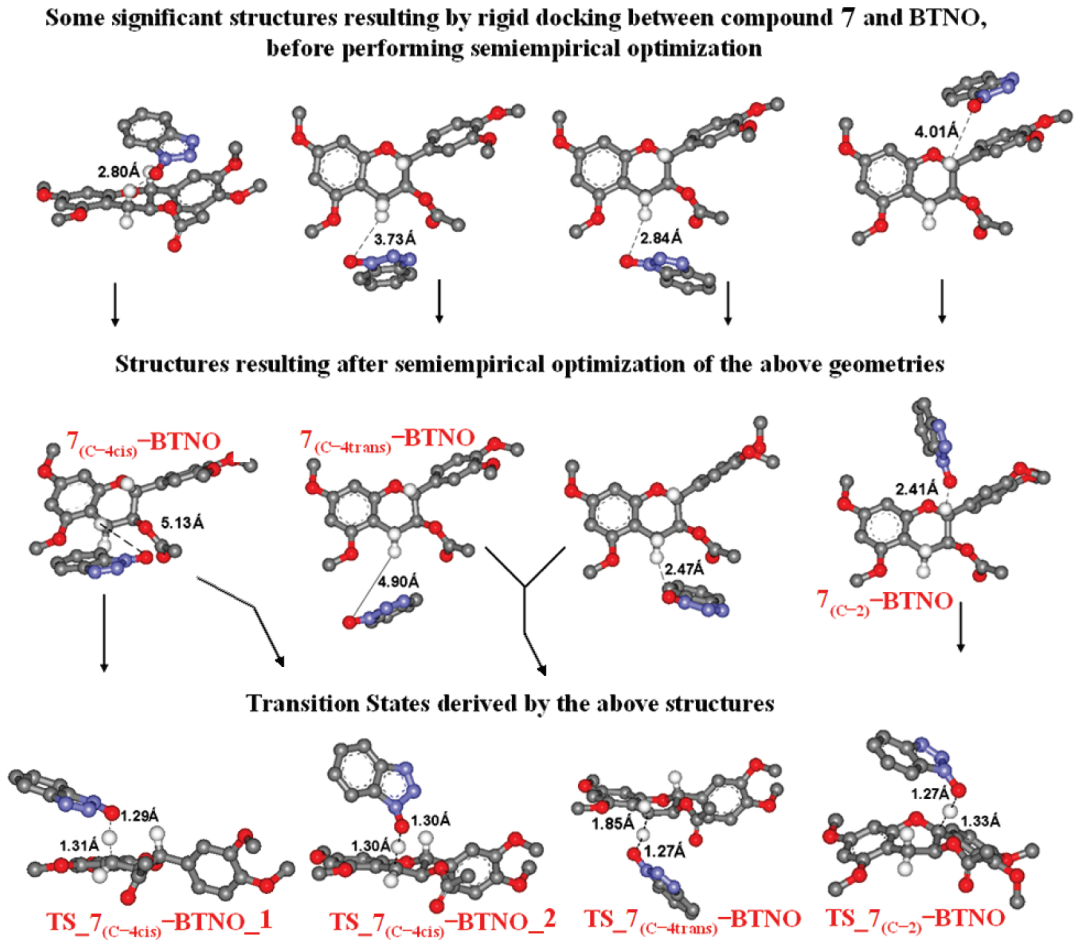

FIGURE 6. Geometries of adducts between 3-*O*-acetyl-catechin 5,7,3′,4′-tetramethyl ether **7** and BTNO, obtained by docking simulation, and related transition states for the hydrogen transfer from catechin to BTNO. For clarity, the only hydrogen atoms shown in the figure are those bonded to carbons C-2 and C-4.

As previously found for the oxidation of catechin derivative **3**, the evaluation of the differential activation energy $\Delta\Delta E^{\#}$ by single point energy DFT calculations related to the generation of radicals at carbons C-4 and C-2 of **7** allowed a logical interpretation of the experimental findings. A very large energetic gap, greater than 39 kJ/mol, was in fact calculated in favor of the H-abstraction from the C-4 benzylic carbon.

By looking for the structural and energetic reasons responsible for the calculated chemoselectivities on catechin derivatives **3** and **7**, we performed some final computational evaluations. The structures of the couple of transition states TS_**3**$_{(C\text{-}4)}$-BTNO_1 and TS_**3**$_{(C\text{-}2)}$-BTNO were deprived of the BTNO component and submitted to single point energy DFT calculations, at the lower level B3LYP/6-31G(*). In addition, from their unmodified geometries were also computed the relevant electrostatic potential surfaces. Forward, the same procedure of calculus was applied to the couple of transition states related to catechin **7**, the geometries TS_**7**$_{(C\text{-}4cis)}$-BTNO_1 and TS_**7**$_{(C\text{-}2)}$-BTNO. For compound **3** it resulted that, at the opposite of the predicted chemoselectivity (hydrogen abstraction from C-4 favored by 11.3 kJ mol^{-1}, Table 4) the arising radical at carbon C-2 was more stable than that at carbon C-4 by 5.9 kJ mol^{-1}. This means that the differential intermolecular interactions involved in the reported chemoselectivity on **3** amount to 17.2 kJ mol^{-1} in favor of the TS_**3**$_{(C\text{-}4)}$-BTNO_1 transition state. By looking at the electrostatic potential surfaces surrounding the TS structures of **3** (Figure 7), at least a quote of such an energetic contribution can be attributed to electrostatic interactions more favorable to the hydrogen abstraction from C-4.

More in particular, in the TS related to the incipient C-2 radical the aromatic framework of BTNO results faced against a molecular portion of catechin endowed with charge of the same sign, which certainly leads to a growth of the related structure energy. A quite similar situation also can be evinced from the relevant analysis of the electrostatic potential surfaces surrounding the transition states structures of **7**. For this compound, however, a completely different contribution from the conformational properties of the incipient C-2 and C-4 radicals was assessed. In this case, in fact, DFT calculations indicated a marked energetic advantage for the arising radical at the carbon C-4 (15.9 kJ mol^{-1}), as in its regioisomeric counterpart (i.e., TS_**7**$_{(C\text{-}2)}$-BTNO) it may be clearly evidenced a meaningful disadvantageous loss of catechin planarity. Such a distortion is evidently induced by steric repulsion from the approaching BTNO. Interestingly, the differential intermolecular interactions related to the chemoselective generation of radical from **7** amounts to

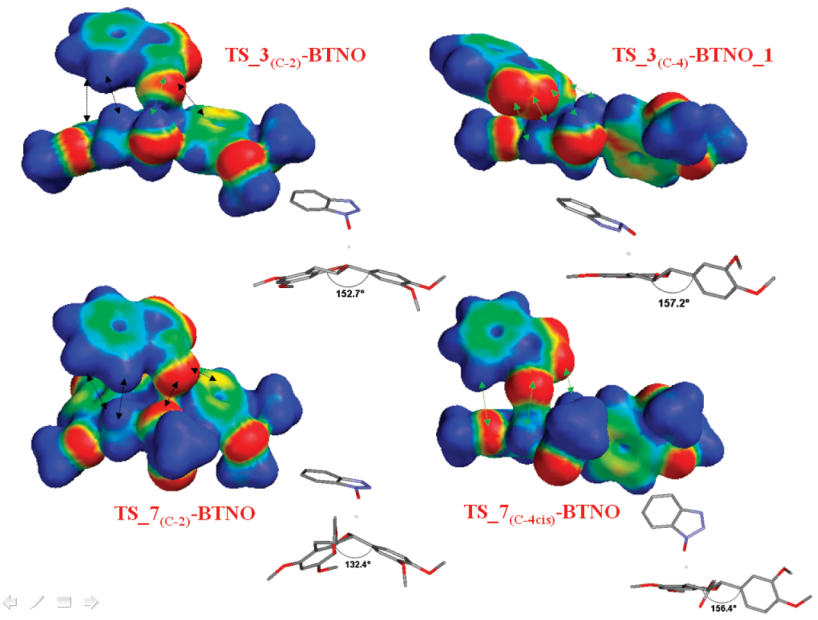

FIGURE 7. Electrostatic potential surfaces surrounding the TS of catechin derivatives **3** and **7**. The extent of distortion from planarity of the catechin units is reported at the bottom-right side of each TS structure. Green arrows refer to attractive electrostatic interactions while black arrows to repulsion forces.

21.3 kJ mol^{-1}, a quote similar to that assessed for catechin 5,7,3′,4′-tetramethyl ether **3**.

In conclusion, assessments of BDE values, k_H, pointed out that the observed chemoselectivity cannot be simply explained in terms of a greater thermodynamic stability of catechin radicals at carbons C-4. Indeed, a rationalization of the experimental data was achieved by evaluating the differential activation energy involved by the H-abstraction from the catechin carbons C-2 and C-4. Both conformational and electrostatic factors were found to play a sensible role in influencing the rate of formation of the considered radicals.

Experimental Section

Materials and Instruments. All chemicals were of the highest commercially available quality and were used as received. Crude laccase from *Trametes villosa* (Novozym 51002) was a gift from Novo Nordisk Co. and was free of lignin or manganese peroxidases. ^{1}H NMR and ^{13}C NMR spectra were recorded on a spectrometer 200 MHz with $CDCl_3$ and CD_3OD as solvents. All chemical shifts are expressed in parts per million (δ scale) and coupling constants in hertz (Hz). Gas chromatographic analyses (GC-MS) were performed on an instrument equipped with 5% phenyl silicone capillary column (30 m × 0.25 mm × 25 μm) and coupled to a MSD instrument operating at 70 eV. HPLC analysis was performed with a C-18 column (150 mm × 4.6 mm × 5 μm) and a UV detector. The kinetic studies were performed with a stopped flow instrument interfaced to a diode array spectrophometer having a thermostated cuvette holder. A conventional UV−vis spectrophotometer was used as an alternative.

Oxidation of Catechin Derivatives with Laccase in Buffered Water/1,4-Dioxane: General Procedure. Oxidation reactions were performed in air at 25 °C in magnetically stirred 1:1 buffered water (pH 4.7, 0.1 M NaOAc)/1,4-dioxane. Catechin derivative (60 μmol) was solubilized in 3.0 mL of reaction medium, followed by the addition of HBT (60 μmol) and laccase (10 U). Additional aliquots of laccase were added every 3 h up until 70 U. The reactions were monitored by thin layer chromatography. At the end of the experiment (24−50 h), the internal standard (1-methyl-6-methoxy-3,4-dihydro-1*H*-isochromen-7-ol **19**, 60 μmol) was added. The mixture was extracted with ethyl acetate; the organic phases were washed with a saturated solution of NaCl and dried over Na_2SO_4. The quantitative yields of the oxidation reactions were determined by HPLC analysis with the internal standard method; suitable response factors were determined from authentic products. Samples were eluted at a flow rate of 1.0 mL/min with the following method: acetonitrile/water = 90/10 (0−10 min); linear gradient until a ratio of acetonitrile/water = 60/40 (10−25 min); acetonitrile/water = 60/40 (5 min); linear gradient until a ratio of acetonitrile/water = 80/20 (30−35 min); and finally acetonitrile/water = 80/20 (5 min).

Kinetic Procedure. BTNO radical was generated in acetonitrile in a thermostated quartz cuvette (optical path 1 cm) by adding a 0.5 mM solution of CAN to a 0.5 mM solution of HBT. A broad absorption band developed immediately (8 ms) in the λ = 350−600 nm region (λ_{max} at 474 nm, ε = 1840 M^{-1} cm^{-1}). The rate of decay was unaffected by the use of degassed acetonitrile. Rate constants of H-abstraction from compounds **3**, **4**, **7**, **14**, and **15** were determined at 25 °C in acetonitrile by following the decrease of the absorbance at λ = 474 nm of BTNO. The initial concentrations of the substrate were in the 5×10^{-3} to 40×10^{-3} M range to enable a pseudo-first-order treatment of the kinetic data. A first-order exponential was a good fit for plots of $(A_t - A_\infty)$ vs time over more than three half-lives; the rate constants (k') were obtained. From a plot of four to five k' vs [substrate]$_o$ data pairs, the second-order rate constant of H-abstraction (k_H) was obtained.

Cyclic Voltammetry. The electrochemical equipment consisted of a computer-controlled in-house potentiostat with a

Vernier Software Multi Purpose Laboratory Interface (MPLI) program for Windows. The three electrodes consisted of a glassy-carbon disk (diameter of 1 mm) working electrode, an Ag/AgCl/KCl 3 M reference electrode ($E°$ vs NHE = $E°$ vs Ag/AgCl + 0.221), and a Pt auxiliary electrode (1 cm^2). All scans were obtained at room temperature. The cyclic voltammetry scans of 2.0 mM of catechin derivatives **3**, **4**, or **7** in acetonitrile solution containing 0.1 M Bu_4NBF_4 as supporting electrolyte were run at a rate of 0.5 V/s.

Computational Methods. All calculations were performed with software packages running on a PC equipped with a 3.40-GHz Intel Pentium 4 CPU, 2 GB of RAM, and OS Windows 2000 Professional. All optimizations of geometries of ground states, radicals, and transition states were performed by the computer program SPARTAN 04 (Wave function, Inc., Irvine, CA). All details regarding the performed calculations are reported in Supporting Information.

Acknowledgment. The authors are grateful to Dr. Chiara Fantera for preliminary results generated during the course of her degree and Prof. Anna Maria Garzillo for helpful discussions on *Trametes trogii* laccase (data not reported).

Supporting Information Available: Purification of laccase, preparation and ^1H, ^{13}C NMR spectral data of all compounds, computational methods, and Cartesian coordinates of all structures reported in Tables 2 and 4. This material is available free of charge via the Internet at http://pubs.acs.org.